Spectral-Like Accuracy in Space of a Meshless Vortex Method

L.A. Barba

Department of Mathematics, University of Bristol, University Walk, Clifton, Bristol BS8 1TW, U.K.; E-mail: l.a.barba@bristol.ac.uk

Abstract. The convergence of a meshless vortex method is studied numerically. The method uses core spreading for diffusion and radial basis function interpolation for spatial adaption of the Lagrangian particles. Spectral accuracy in space is observed in the absence of convection error, and second order of convergence is obtained it its presence.

Key words: Vortex method, radial basis functions, convergence.

1 Introduction

We consider the accuracy and convergence of a meshless method for fluid dynamics based on vortex particles. The vortex method has a long history, beginning with the use of point vortices to study the instability of a vortex sheet [14]. Although many important achievements have been produced since, there continue to be some frustrations. In fact, the vortex method is still viewed in some circles as a modelling approach and not as direct simulation. The following opinion, expressed some years ago, is relevant today: "*There has been and perhaps there will always be some skepticism about the use of vortices for flow simulation*" [18]. For this reason, it is important to make contributions to the validation and verification of vortex method codes, and this work is a step in that direction.

The vortex method solves the Navier–Stokes equation in vorticity formulation,

$$\frac{\partial \boldsymbol{\omega}}{\partial t} + \mathbf{u} \cdot \nabla \boldsymbol{\omega} = \boldsymbol{\omega} \cdot \nabla \mathbf{u} + \nu \Delta \boldsymbol{\omega} \tag{1}$$

by discretizing the vorticity field into smooth Lagrangian particles:

$$\boldsymbol{\omega}(\mathbf{x}, t) \approx \boldsymbol{\omega}^h(\mathbf{x}, t) = \sum_{i=1}^{N} \boldsymbol{\Gamma}_i(t) \zeta_\sigma \left(\mathbf{x} - \mathbf{x}_i(t)\right) . \tag{2}$$

V.M.A. Leitão et al. (eds), Advances in Meshfree Techniques, 187–197.

Here, $\mathbf{\Gamma}_i$ is the vector circulation strength (a scalar in 2D) of a vortex particle located at $\mathbf{x}_i$. The particle's vorticity distribution function, ζ_σ , often called the cutoff function, can be for example a Gaussian; in two dimensions:

$$\zeta_\sigma(\mathbf{x}) = \frac{1}{2\pi\sigma^2} \exp\left(\frac{-|\mathbf{x}|^2}{2\sigma^2}\right). \tag{3}$$

The particles are evolved by integrating their trajectories with the velocity at their center, evaluated using the Biot–Savart law, which in 2D is:

$$\mathbf{u}(\mathbf{x}, t) = \frac{-1}{2\pi} \int \frac{\left(\mathbf{x} - \mathbf{x}'\right) \times \omega(\mathbf{x}', t)\hat{\mathbf{k}}}{|\mathbf{x} - \mathbf{x}'|^2} d\mathbf{x}'. \tag{4}$$

Using the discretized form of the vorticity, Equation (2), in the Biot–Savart law, the discretized velocity is obtained. The Gaussian cutoff function allows the integral in (4) to be evaluated analytically, after which the velocity at one particle's location is obtained by summing the influence over all others. Clearly, the direct evaluation of the discrete velocity is an N-body problem, for which reason the computational efficiency can be greatly improved using a fast multipole method [10]. Once the velocity is computed, the vortex method is expressed in the following system of equations:

$$\frac{d\mathbf{x}_i}{dt} = \mathbf{u}(\mathbf{x}_i, t) \tag{5}$$

$$\frac{d\omega}{dt} = \nu\nabla^2\omega + \text{ B.C.} \tag{6}$$

The above equations express the fact that the vorticity transport is solved by moving the vortex-particle elements with the local velocity of the fluid. This is the only part of the vortex method that is required for ideal flow. For viscous flow, the method has been extended by providing a change in vorticity at the vortex particles due to the viscous effects. This is generally accomplished in a split-step formulation. In addition, the presence of boundaries in the flow can also be translated into changes in the vorticity, which is expressed by the term "B.C." in Equation (6).

The variety of schemes used in vortex methods to provide viscous effects are reviewed in [6]. In this work, we have used the core spreading method, in which particle core sizes are grown to exactly solve the diffusion part of the equation [12]. The representative length scale of the computational vortex elements, σ, is made to grow according to the following equation:

$$\frac{d\sigma^2}{dt} = 2\nu, \tag{7}$$

Note that this scheme is exact in its representation of the viscous effects, due to the fact that the Gaussian function is an exact solution of the heat equation. It is

important to realize that this method is formulated specifically for the Gaussian cutoff in two dimensions. Some authors have neglected this fact, resulting in applications of questionable consistency [3].

The core spreading method is fully localized and grid-free; however, it requires core size control to tackle consistency issues brought up in [9]. Simply stated, the characteristic length scale of the computational particles cannot be allowed to grow uncontrolled, as they represent the smallest resolved scales. The consistency problem arises due to the fact that the Gaussian elements are convected without deformation. In the present vortex method, control of the particle sizes is provided in a spatial adaption algorithm using radial basis function interpolation, as described later.

The rest of the paper will present a discussion of the discretization accuracy of the vortex method, and in particular the so-called "convection error" of the Lagrangian formulation (Section 2), and subsequently a report of numerical convergence studies performed using a parallel implementation of the method described in [6]. We use both axisymmetric test flows (for which an analytic solution allows precise error measurements) and non-axisymmetric tests, which are more challenging.

The vortex method with core spreading for diffusion, and a spatial adaption process that uses radial basis function (RBF) interpolation, was implemented in parallel using the PETSc library [1] in a C++/MPI code. In this implementation, the RBF interpolations are solved using the built-in pre-conditioners and GMRES solver of PETSc. More details of the parallel implementation are given in [2].

2 Discretization Accuracy of the Vortex Method

The Lagrangian approach described above is devoid of numerically diffusive truncation errors, which makes the vortex method especially suited for the study of high-Reynolds number vortical flows.

This often praised feature of Lagrangian particle methods too frequently remains unexplained. The low numerical dissipation of the vortex method arises from the fact that the nonlinear term in the Navier–Stokes equation is replaced by a set of ordinary differential equations for the particle locations. As a result, the equivalent of a local truncation error for the vortex method is what is called "convection error" in the specialized literature.

Convection error in vortex methods refers to the error which originates from convecting the vortex particles without deformation with the velocity at their centers. A derivation of the estimate for this error when using Gaussian particles is presented in [12]. The estimate is obtained by subtracting the discrete representation of the velocity to the exact velocity in the nonlinear convective term, as follows:

$$\varepsilon(\mathbf{x}) = \nabla \cdot \left[\sum_{i=1}^{N} \Gamma_i \ \zeta_\sigma(\mathbf{x} - \mathbf{x}_i) \left(\mathbf{u}(\mathbf{x}) - \frac{d\mathbf{x}_i}{dt} \right) \right] \tag{8}$$

which, after a Taylor expansion and some algebra results in the following estimate:

$$\varepsilon(\mathbf{x}) = \sigma^2 \frac{\partial^2 \omega}{\partial x_j \partial x_k} \frac{\partial u_j}{\partial x_k}. \tag{9}$$

Thus, one sees that this error is second order in σ and that it does not diffuse vorticity. The result in (9) also indicates that axisymmetric flows do not suffer from convection error, as only the symmetric part of the velocity gradient tensor has a contribution, hence the result of (9) in principal coordinates is zero for axisymmetric flow. This observation is important to have in mind, as the use of axisymmetric test problems for validation of vortex method codes is widespread practice.

In addition to convection error, the vortex method suffers from an increase of the spatial discretization error over time, due to the vortex particles becoming disordered. In the sense of function approximation, the spatial discretization using particles depends on a measure of the particle density: smooth particles need to overlap at all times to be able to represent a continuous field. As particles follow the flow map, there is a chance of gaps appearing in the particle distribution, or particles clustering together in other areas. This problem must be corrected with a scheme that adapts the particle in such a way that overlap is always maintained, and clustering avoided.

The standard solution to this situation is applying a remeshing scheme, as introduced in [11]. This has allowed long-time calculations with the vortex method by effectively controlling the growth of discretization error, but at the cost of introducing some numerical dissipation and grid-dependency. Remeshing schemes are based on tensor product formulations, and are subject to interpolation errors.

An alternative to the standard remeshing schemes is using radial basis function (RBF) interpolation techniques in a fully meshless spatial adaption process; the method is introduced and described in detail in [6]. It is basically a way to rediscretize the vorticity field with a set of new vortex particles that are well-overlapped and represent accurately the current flow field.

When interpreting the spatial discretization of the vortex method as an approximation problem using RBFs, one can see the potential for spectral-like accuracy in space. It has been established that RBF interpolation has spectral accuracy when using Gaussian bases [19].

In this paper, we show numerical experiments that confirm spectral accuracy in a vortex method in the absence of convection error. It is noteworthy that this result is obtained in a *viscous* calculation, showing that core spreading does not limit the accuracy that can be obtained from the vortex method (unlike other viscous approaches; for example, the particle strength exchange method [8] is limited to second order accuracy, and deteriorates as particles become disordered).

Convection error, however, will be present in the general case. Further numerical experiments presented here verify *observed* second order accuracy in the presence of convection error when using Gaussian bases. Hence, the possibility of increasing the

convergence rate now lies in reducing convection error, perhaps by using deformable basis functions or some other approach.

3 Numerical Convergence Study

3.1 Axisymmetric Test Flow

A first convergence study is performed using an axially symmetric viscous flow, for which an analytic solution is available. This is the Lamb–Oseen vortex, for which the vorticity evolves as follows, with $r = x^2 + y^2$:

$$\omega(r, t) = \frac{\Gamma_0}{4\pi\nu t} \exp\left(-\frac{r^2}{4\nu t}\right). \tag{10}$$

Here, Γ_0 represents the total circulation of the vortex, and ν is the fluid viscosity. The Lamb–Oseen vortex simply spreads over time, while the maximum vorticity decreases, in a self-similar way.

To minimize time-stepping errors in these numerical tests, a very small time step was used of $\Delta t = 0.002$ in a 4th order Runge–Kutta scheme. The calculations were advanced for 200 time steps, and spatial adaption was performed every 5 steps. Although no regular particle arrangement is required by the formulation, the particles were placed in a triangular lattice, covering the vorticity support to a minimum circulation level of 10^{-10} (i.e., after spatial adaption, particles with $\Gamma_i < 10^{-10}$ are deleted).

Several initial values of the inter-particle spacing h were chosen, and a run was performed for each value. Then for each run, the pointwise errors were measured at each time step, using the maximum norm. The largest value of the error in the time-marching calculation was used for each run to produce the plot in Figure 1. As shown by the functional fit added in the plot, the results of this numerical convergence study are consistent with the spectral convergence of radial basis function interpolation using Gaussians. Note that the measure of error chosen for the plot is the maximum in both space and time, for each run. The curve slopes off around the level 10^{-10}, which is probably a result of our population control scheme (mentioned above).

A similar result to the one presented in Figure 1 was included in [6], but for stationary tests (no time stepping). There, it was simply a case of proving that the discretization of the vorticity field using vortex particles could exhibit spectral convergence. Here, we have incorporated time marching, with periodic spatial adaption using radial basis functions, in a viscous calculation.

The numerical convergence result of Figure 1 likely shows the best accuracy that can be obtained with the vortex method. This is because the Lamb–Oseen vortex flow is a benign test, due to its infinite smoothness and more importantly to its immunity

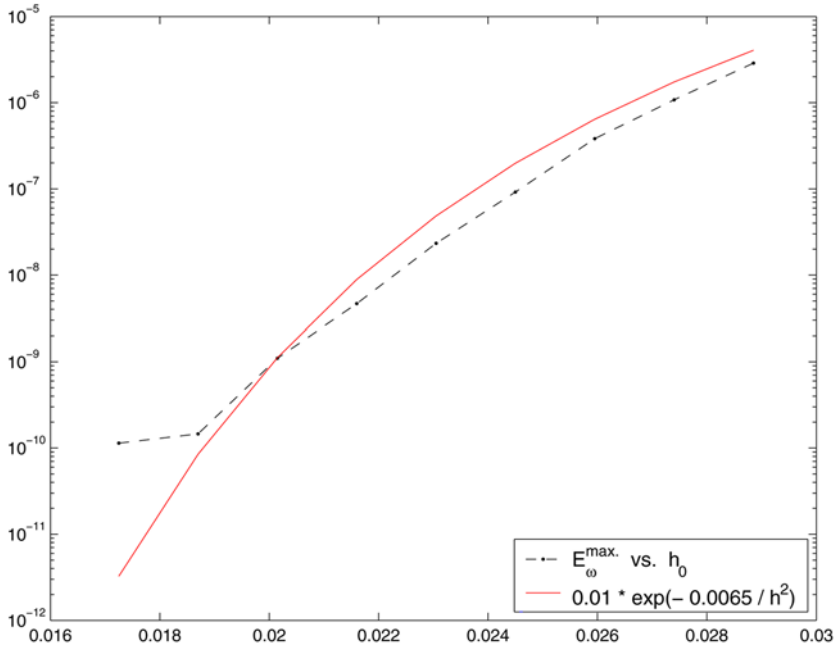

Fig. 1. Plot of the maximum vorticity errors during 200 time steps vs. the inter-particle spacing h and an exponential fit to the error behavior.

to convection error. Nonetheless, it is an important result because it demonstrates that the RBF-based spatial adaption scheme does not limit the accuracy of the vortex method. This is in contrast to the standard remeshing schemes, based on tensor products of 1D kernels (which furthermore require a Cartesian grid). It has been recognized that the remeshing schemes do introduce some error; these were clearly displayed in numerical experiments presented in [5].

Note again that the results above are produced by a *viscous* vortex method. The use of core spreading with adequate core size control, therefore, does not slow the rate of convergence of the spatial discretization. The core size control is provided here in the RBF interpolation step, where the core sizes can be reset to any desired value. This automatic form of core size control does not have an effect on the accuracy, unlike the vortex splitting technique of [15], which is numerically diffusive.

3.2 Non-Axisymmetric Test Flow

Next, a convergence study is presented using a non-axisymmetric flow, and thus subject to convection error. The initial vorticity consists of a quadrupole perturbation ω' on a Gaussian vortex ω_o, resulting in localized elliptical deformation of the core, and

an evolution that develops filaments and exhibits a quasi-steady tripole for large amplitude of the perturbation. This flow was studied in [17], and used as proof-of-concept for the vortex method developed in [2]. Furthermore, detailed parameter studies for this flow problem have been performed recently [4]. The initial conditions are obtained from the superposition of an axisymmetric eddy and the non-axisymmetric perturbation, as $\omega = \omega_o + \omega'$:

$$\omega_o(\mathbf{x}) = \frac{1}{4\pi} \exp\left(\frac{-|\mathbf{x}|^2}{4}\right), \quad \omega'(\mathbf{x}) = \frac{\delta}{4\pi} |\mathbf{x}|^2 \exp\left(\frac{-|\mathbf{x}|^2}{4}\right) \cos 2\theta. \tag{11}$$

For the present calculations, the Reynolds number is 1000, defined as $Re = \Gamma/\nu$, and the amplitude of the perturbation is $\delta = 0.25$.

The use of a non-axisymmetric test problem to perform convergence studies is usually hampered by the lack of an analytical solution. But, as explained in [13], it is possible to extract the *observed order of convergence* from a grid-convergence study, using three grid solutions. This verification technique was of course developed for grid-based methods, but there is not obstacle to applying the same concepts in a meshless method, if one uses an equivalent measure of "grid-refinement".

The technique is as follows: if one obtains three numerical solutions of a given problem with the same code, using three different spatial discretizations given by h_1, h_2, and h_3 with a fixed grid-refinement ratio $r = h_3/h_2 = h_2/h_1$ (the subscript 1 refering to the finest resolution), then one can obtain an *empirical* convergence order p by the following relation:

$$p = \ln\left(\frac{u_{h_3} - u_{h_2}}{u_{h_2} - u_{h_1}}\right) \Big/ \ln(r). \tag{12}$$

In the case of the vortex particle method, we take as the resolution parameter the initial inter-particle spacing, at the time of discretization. In reality, the vortex method has two resolution parameters: the inter-particle spacing, and the overlap ratio (defined as the inter-particle spacing divided by the particle size). We chose to leave the value of the overlap ratio unchanged for this study, and thus base the refinement study on the inter-particle spacing. Moreover, as the discretization used is based on placing the vortex particles on a triangular lattice, we use a measure h which corresponds to the equivalent square lattice, providing the same cell area as in the triangular lattice used.

Three solutions were computed of the flow with initial vorticity as in (11), with a grid-refinement ratio of $r = 1.4$. The runs were carried for 740 time steps, with $\Delta t = 0.05$. The vorticity was sampled on the same mesh for all runs, corresponding to the finer value of h. Spatial adaption was performed every 10 steps with the same procedure described before, using radial basis function interpolation. Table 2, below, shows the problem sizes for this convergence study, in terms of the total number of vortex particles needed to cover the vorticity support down to a level of particle circulation of 10^{-10}.

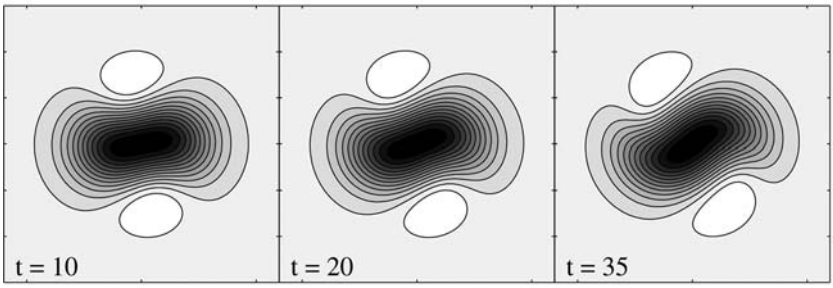

Fig. 2. Vorticity contours for the non-axisymmetric test flow, at the times used for the convergence study. Note that the white filled contour corresponds to negative inclusions in the vorticity field. This flow is undergoing a markedly non-steady re-organization of vorticity.

Table 1. Problem sizes for convergence study runs.

particle spacing	$N(t=0)$	$N(t=37)$
$h_1 = 0.09$	20389	21978
$h_2 = 0.126$	10361	11418
$h_3 = 0.1764$	5309	5957

Table 2. Observed order of convergence for time-marching runs.

time-slice \ norm used:	$E_\omega^{L^2}$	$E_\omega^{\text{rel,max}}$
$t = 10$	2.0282	2.0271
$t = 20$	2.026	2.027
$t = 35$	2.0175	2.0191

By means of a comparison of the point-by-point value of vorticity at each three time-slices, $t = 10, 20, 35$, and taking both a discrete L^2-norm and a maximum norm (normalized by the maximum vorticity), measurements of the observed order of convergence were performed by applying (12). The results are presented in Table 2, where the table values correspond to the computed value of p.

The results above are perhaps surprisingly consistent, giving an observed second-order of convergence. Since the principal difference between this test problem, and the Lamb–Oseen vortex used previously is the lack of axisymmetry in the present case, we conclude that the observed order of convergence is fundamentally due to convection error.

In other words, the vortex method exhibits spectral order of convergence in the spatial discretization, as demonstrated in the experiments of Section 3.1, but in a time-marching algorithm it is limited by the second order of the convection error.

This result is specific for the second order Gaussian cutoff used in the particle discretization of *these* simulations, however. There have been several proposals for using higher-order cutoff functions, but as shown in practice by the numerical experiments in [5], higher-order cutoffs are more sensitive to overlap, and thus require more frequent spatial adaption. This results in a considerable penalty, to the point that some authors opt for spatially adapting on *every* time step. Another means of achieving higher-order with the vortex method including convection error is the use of deformable basis functions; the recent work of Rossi [16] demonstrates fourth-order accuracy with elliptical Gaussian bases.

As a final note, we add that the theory of convergence of vortex methods (see [7] for details and further references) establishes second order convergence when using a Gaussian cutoff. However, the analysis assumes a standard initialization based on the local vorticity value multiplied by h^2 on a Cartesian grid, as an estimate of the particle circulation strengths. Thus, initialization of the method is already limited to second order. Using instead RBF interpolation to obtain the initial particle circulations allows for spectral accuracy in space in the absence of convection.

4 Conclusion

Extensive numerical experiments performed previously [2], both with standard remeshing and with the radial basis function interpolation, demonstrate that the remeshing schemes impose an accuracy limitation on the vortex method. By using instead radial basis function interpolation, the accuracy limitation of the spatial adaption process is removed, and convection error is left to dominate on the rate of convergence. We have demonstrated using numerical experiments that in the absence of convection error, spectral accuracy is possible is space. With convection error being present in a non-axisymmetric unsteady flow, we have shown by means of a refinement study an observed second order of convergence of the method. This result is a manifestation of the convection error produced when using simple Gaussians as basis functions. Higher order vortex methods are thus possible with techniques to reduce convection error, such as using deformable basis functions. Two important implications of the present study are the fact that there is no accuracy limitation imposed by the method used for spatial adaption, as radial basis function interpolation is spectral order, and that the viscous scheme of core spreading is also able to preserve the high accuracy and convergence.

Acknowledgements

Computations were carried out in the Beowulf cluster of the Laboratory for Advanced Computation in the Mathematical Sciences, University of Bristol

(http://lacms.maths.bris.ac.uk/). Thanks to Tony Leonard for many helpful discussions and thanks to the PETSc team for prompt and helpful technical support. The author's travel was made possible by a grant from the Nuffield Foundation.

References

1. S. Balay, K. Buschelman, W. D. Gropp, D. Kaushik, M. Knepley, L. Curfman-McInnes, B. F. Smith, and H. Zhang. PETSc User's Manual. Technical Report ANL-95/11 – Revision 2.1.5, Argonne National Laboratory, 2002.
2. L. A. Barba. *Vortex method for computing high-Reynolds number flows: Increased accuracy with a fully mesh-less formulation*. PhD Thesis, California Institute of Technology, 2004.
3. L. A. Barba. Discussion: Three-dimensional vortex method for gas-particle two-phase compound round jet (Uchiyama, T., and Fukase, A. 2005 ASME J. Fluids Eng., 127, pp. 32–40). *J. Fluids Eng.*, 128:643–645, May 2006.
4. L. A. Barba and A. Leonard. Emergence and evolution of tripole vortices from non-shielded initial conditions. Submitted, 2006.
5. L. A. Barba, A. Leonard, and C. B. Allen. Numerical investigations on the accuracy of the vortex method with and without remeshing. AIAA #2003-3426, 16th CFD Conference, Orlando FL, June 2003.
6. L. A. Barba, A. Leonard, and C. B. Allen. Advances in viscous vortex methods – Meshless spatial adaption based on radial basis function interpolation. *Int. J. Num. Meth. Fluids*, 47(5):387–421, 2005.
7. G.-H. Cottet and P. Koumoutsakos. *Vortex Methods. Theory and Practice*. Cambridge University Press, 2000.
8. P. Degond and S. Mas-Gallic. The weighted particle method for convection-diffusion equations. Part 1. The case of an isotropic viscosity. *Math. Comp.*, 53:485–507, 1989.
9. C. Greengard. The core spreading vortex method approximates the wrong equation. *J. Comp. Phys.*, 61:345–348, 1985.
10. L. Greengard and V. Rokhlin. A fast algorithm for particle simulations. *J. Comp. Phys.*, 73:325–348, 1987.
11. P. Koumoutsakos. Inviscid axisymmetrization of an elliptical vortex. *J. Comp. Phys.*, 138:821–857, 1997.
12. A. Leonard. Vortex methods for flow simulation. *J. Comp. Phys.*, 37:289–335, 1980.
13. P. J. Roache. Quantification of uncertainty in computational fluid dynamics. *Ann. Rev. Fluid Mech.*, 29:123–160, 1997.
14. L. Rosenhead. The formation of vortices from a surface of discontinuity. *Proc. R. Soc. Lond. A*, 134:170–192, 1931.
15. L. F. Rossi. Resurrecting core spreading vortex methods: A new scheme that is both deterministic and convergent. *SIAM J. Sci. Comput.*, 17:370–397, 1996.
16. L. F. Rossi. Achieving high-order convergence rates with deforming basis functions. *SIAM J. Sci. Comput.*, 26(3):885–906, 2005.
17. L. F. Rossi, J. F. Lingevitch, and A. J. Bernoff. Quasi-steady monopole and tripole attractors for relaxing vortices. *Phys. Fluids*, 9:2329–2338, 1997.

18. T. Sarpkaya. Computational methods with vortices. *J. Fluids Eng.*, 11:5–52, 1989.
19. R. Schaback. Improved error bounds for scattered data interpolation by radial basis functions. *Math. Comp.*, 68(225):201–216, 1999.